FORCED NONLINEAR MAGNETIC RECONNECTION

H.J. de Blank, J. Rem, and G. Valori

FOM-Instituut voor Plasmafysica, Association Euratom-FOM,
Trilateral Euregio Cluster, P.O. Box 1207, 3430 BE Nieuwegein, The Netherlands

1. Introduction

Reconnection of magnetic fields in plasmas is associated with such different phenomena as solar flares, events in the Earth magnetotail, and the formation of stochastic magnetic fields in laboratory plasmas. Reconnection processes in high temperature plasmas have received much consideration in thermonuclear fusion research, because reconnecting instabilities are thought to cause the disruptive relaxation of tokamak plasmas: the sudden loss of particles and energy occurs only after the breakup of initially closed magnetic surfaces.

Under many circumstances, *e.g.* in internal disruptions in sufficiently hot tokamak plasmas, reconnection takes place on a time scale that is short compared to the resistive time [1]. In such cases, electron inertia can decouple the plasma motion from the magnetic field. The resulting collisionless reconnection may account for the observed fast reconnection rates. A striking effect of electron inertia is the formation of a current density sublayer narrower than the inertial skin depth $d_e = c/\omega_{pe}$ [2][3].

Another parameter which has a profound influence on the narrow current sublayer is the ion sound gyroradius $\rho_s = \sqrt{T_e/m_i}/\omega_{ci}$. This length scale arises in a two-fluid model due to coupling of the parallel electron compressibility to the ion motion, via the Hall term in the generalized Ohm's law.

The non-linear evolution of the current density sublayer is the focus of this paper. We shall demonstrate analytically and numerically that the ρ_s-term causes a collapse of the current sublayer within a finite time, leading to singular distributions of the current density and vorticity. The singularity arises in the cases of collisional as well as collisionless reconnection.

2. Model equations

Our model is based on the extension of reduced MHD to a two-fluid model given in Ref. [4] (a more general model was used in [5]), where the contribution of electron inertia to the generalized Ohm's law provides the mechanism for collisionless reconnection. Also the electron gyroviscosity and the Hall term are retained in the generalized Ohm's law. For the electrons the isothermal equation of state is adopted. This model has a Hamiltonian structure [6], in which three flux densities (combinations of the magnetic flux, electrostatic potential, and density) are frozen in the flow fields of three generalized stream functions.

In this paper a simplification of the model [4] is made by considering the cold ion regime, $\rho_i \equiv \sqrt{T_i/m_i}/\omega_{ci} \ll \rho_s$, thus neglecting ion diamagnetic effects. We expect that the conclusions of this paper can be extended to the finite-T_i case. We extend the model by adding the dissipative effects of the resistivity η and the ion viscosity ν_i (thus spoiling the Hamiltonian structure).

The reduced equations are based on a magnetic field with a dominant, constant, component in the z-direction, $\mathbf{B} = B_0(\mathbf{e}_z + \mathbf{e}_z \times \nabla\psi)$. The electric field is $\mathbf{E} = B_0(-\nabla\phi + \mathbf{e}_z\partial\psi/\partial t)$, where ψ and ϕ are the normalized flux and scalar potential. Let j and ω be the z-components of

the current density and vorticity. We have set one of the three conserved scalar functions equal to zero by fixing the density perturbations to $\log n = \omega/\omega_{ci}$. The following set of equations is derived,

$$\psi_t - d_e^2 j_t = -[\phi, \psi - d_e^2 j] + \rho_s^2[\omega, \psi] + \eta j, \tag{1}$$

$$\omega_t = -[\phi, \omega] + [\psi, j] + \nu_i \Delta\omega, \tag{2}$$

$$\omega = \Delta\phi, \tag{3}$$

$$j = \Delta\psi. \tag{4}$$

where $[A, B] \equiv A_x B_y - A_y B_x$. Partial derivatives with respect to t, x, and y are indicated by subscripts. In the limit of vanishing dissipation, there are two conserved flux functions $G^{\pm} \equiv \psi - d_e^2 j \pm \rho_s d_e \omega$ that are frozen in the flow fields of the stream functions $\Phi^{\pm} \equiv \phi - \rho_s^2 \omega \pm \rho_s d_e j$,

$$G_t^{\pm} + [G^{\pm}, \Phi^{\pm}] = 0. \tag{5}$$

3. Numerical simulation

We have numerically simulated forced reconnection on the basis of Eqs. (1–4), extending the results of Ref. [7] on forced resistive reconnection to cases including electron inertia and parallel compression.

A rectangular domain $-L_x < x < L_x$, $-L_y < y < L_y$, periodic in y, is used. Starting with stable equilibrium fields ($\phi = 0$ and $\psi = \frac{1}{2}x^2$), an Alfvén wave is excited by specifying $\Phi(y, t)$ at $x = \pm L_x$, approximately modelling moving, ideally conducting, walls with positions $\pm x = L_x + \delta_{\rm wall} \cos(\pi y/L_y) \tanh(t/\tau_{\rm wall})$.

In the linear regime, the different reconnection rates in the resistive and collisionless cases are as expected theoretically. However, nonlinearly, the current and vorticity sheets form new structures, in agreement with those found in Ref. [8]. The current layer width is found to shrink indefinitely within a finite time, *i.e.*, a collapse of length as well as time scales seem to occur. This process takes place below the ρ_s and d_e scales in resistive as well as collisionless reconnection, and is not stopped by ion viscosity. In order to follow the collapsing length scales as far as possible, the numerical simulations used a finite difference scheme with local grid refinement. As an example, we present results obtained without resistivity and viscosity, and with $L_x = 1$, $L_y = 10$, $\delta_{\rm wall} = 0.04$, $d_e^2 = \rho_s^2 = 10^{-3}$, and $\tau_{\rm wall} = 10\tau_A$. In Fig. 1 the functions ψ, j, ω, Φ^+, and G^+ are shown on a narrow strip around $x = 0$ for $t = 93\tau_A$. Shortly after

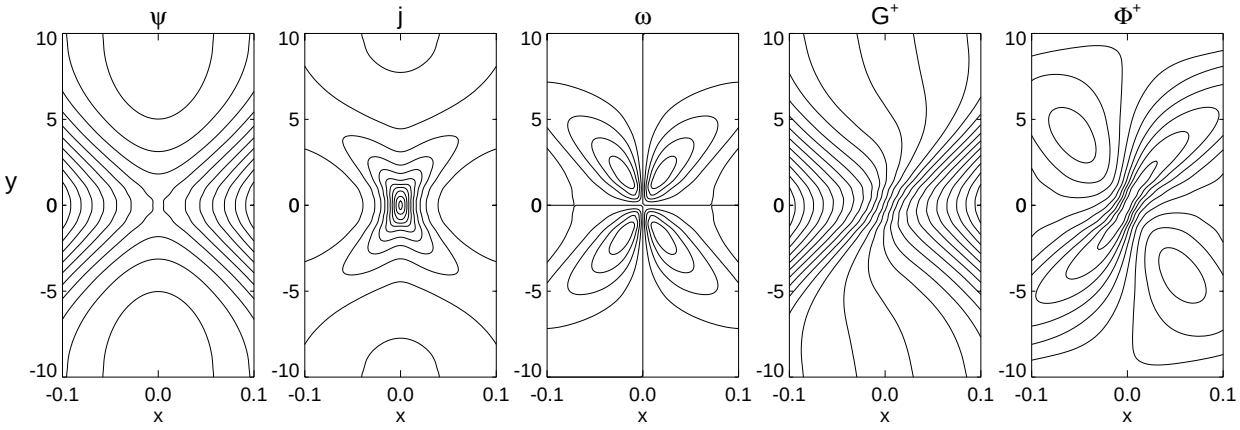

Fig. 1: Contours of the vector potential component ψ, the current density j, the vorticity ω, the conserved scalar field G^+, and the associated stream function Φ^+.

$t = 93\tau_A$ the current distribution became too narrow to be resolved. One sees that X-point formation has taken place in ψ but not in $G^{\pm}$. In this deeply nonlinear regime, the stream function Φ^+ becomes localized along a diagonal channel with an angle depending on d_e and ρ_s.

The current density is a superposition of Φ^+ and its mirror image Φ^-. It therefore obtains the peculiar x-shape shown in the figure, with a narrow central peak. The vorticity also becomes very localized: it is approximately proportional to the difference $\Phi^+ - \Phi^-$.

4. Finite time singularity

We investigate the extreme peaking of the current density and vorticity profiles around the X-point by means of an expansion in small (x, y), making use of the observation from the numerical results that the x-scale is by far the smallest length scale in the system,

$$\frac{\partial}{\partial x} \gg \frac{1}{\rho_s}, \frac{\partial}{\partial y}.$$

Hence, as $\Delta \approx \partial^2/\partial x^2$, ϕ is neglible compared to $\rho_s^2\omega$, and the system is described by the following pair of equations,

$$\psi_t - d_e^2\psi_{txx} = \rho_s^2(\omega_x\psi_y - \omega_y\psi_x) + \eta\psi_{xx}, \tag{6}$$

$$\omega_t = \psi_x\psi_{xxy} - \psi_y\psi_{xxx} + \nu_i\omega_{xx}. \tag{7}$$

The numerical simulations of the full set of equations (1–4) indicate that the ρ_s^2-term is important for the strong nonlinear behaviour: near the X-point, energy from the Alfvén waves is converted into vortical energy, $E_\omega = \int \frac{1}{2}\rho_s^2\omega^2\, d^2x$. We shall now consider the possible singular behaviour at $t \uparrow t_0$, in the form of a power law $\sim \tau^r$, $\tau \equiv t_0 - t$. In the limit $\tau \downarrow 0$ the equations have an isobaric structure, with solutions of the form (p, q, and r are constants)

$$\psi(t, x, y) = \tau^r\psi(x\tau^q, y\tau^p), \qquad \omega(t, x, y) = \tau^{2r+p+3q+1}\omega(x\tau^q, y\tau^p). \tag{8}$$

Collapsing scale lengths correspond to $p, q < 0$. The dissipative terms put constraints $p, q \geq -\frac{1}{2}$ on the singular behaviour. Further constraints on p and q follow by noting that the energy E_ω should remain finite. We consider two limit cases in detail:

case 1: resistive reconnection This case is found in the limit of negligible electron inertia, $x \gg d_e$ and $\psi_t \gg d_e^2 j_t$, so that $r = -p - 2q - 1$. Expanding the solutions ψ and ω as Taylor series in y and subsequently considering the asymptotic behaviour for $x \to \infty$, we find that the dominant terms are

$$\psi(x, y, t) = \sum_{k=\text{even}} \psi_k y^k x^{(p-kp+2q+1)/q}, \qquad \omega(x, y, t) = \sum_{k=\text{odd}} \omega_k y^k x^{(p-kp+q+1)/q}. \tag{9}$$

These expressions show that the solutions are independent of t for large x (as they should be) and that the nonlinear terms, being $\mathcal{O}(x^{1/q}t)$, are negligible for large x. Expressions (8) predict that at the X-point, the vorticity is given by

$$\omega \approx \frac{xy}{\rho_s^2\tau}, \tag{10}$$

independent of p and q. This $1/\tau$ behaviour is confirmed by the simulations of resistive reconnection.

case 2: collisionless reconnection In this case $x \ll d_e$ and, neglecting ψ_t compared to $d_e^2 j_t$, one finds $r = -p - q - 1$ in Eq. (8). The X-point behaviour is

$$j(t, x, y) = \tau^{q-p-1}j(x\tau^q, y\tau^p), \qquad \omega(t, x, y) = \tau^{q-p-1}\omega(x\tau^q, y\tau^p). \tag{11}$$

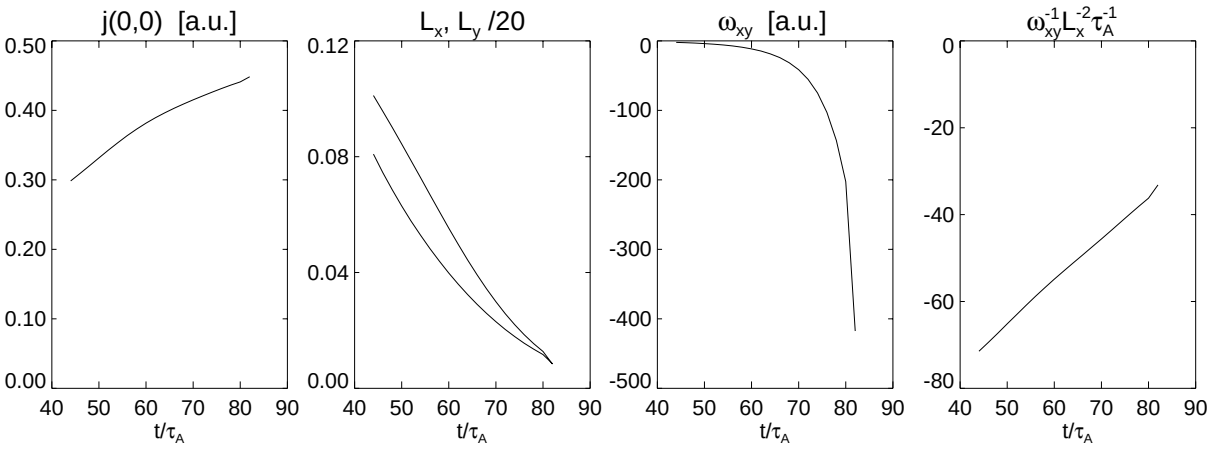

Fig. 2: Time evolution of the central current density j, the $x,\ y$ half-widths (L_x and L_y) of the current peak, and two quantities measuring the vorticity near the X-point. The last graph shows a linear time behaviour $\omega_{xy}^{-1} L_x^{-2} \approx t_0 - t$, as predicted by the scaling for $x \ll d_e$.

Solutions of this form, unlike those in (9), are not regular for $x \to \infty$. This is a consequence of neglecting ψ_t. Contrary to the purely resistive case, the collisionless model has a vorticity scaling near the X-point that depends on the parameter q, $\omega \sim xy\tau^{2q-1}$.

In order to illustrate the temporal behaviour near the X-point singularity, we present numerical results for very large values $d_e = 0.25$ and $\rho_s = 0.18$, and without dissipation. The results are shown in Fig. 2. As measures of the $x,\ y$-scale lengths we have taken the half-widths $L_x,\ L_y$ of the current spike. Then, since $L_x \sim \tau^{-q}$, our analysis predicts $\omega_{xy} L_x^2 \sim \tau^{-1}$. We find a good match with the numerical result.

5. Conclusions

We have numerically simulated forced reconnection of a magnetized plasma slab based on a reduced 2-fluid model, allowing for both collsionless and resistive reconnection. The formation of current and vorticity sublayers at the X-point was studied. The widths of these layers seem to vanish within a finite time. This singular behaviour is consistent with an analytic study of the model equations. Inclusion of the ion and viscosity does not remove the singularity.

Acknowledgements

This work was performed under the Euratom-FOM Association agreement with financial support from NWO and Euratom.

References

[1] J. Wesson: Nucl. Fusion **30**, 2545 (1990).

[2] M. Ottaviani and F. Porcelli: Phys. Rev. Lett. **71**, 3802 (1993).

[3] J.F. Drake and R.G. Kleva: Phys. Rev. Lett. **66**, 1458 (1991).

[4] T.J. Schep, F. Pegoraro, and B.N. Kuvshinov: Phys. Plasmas **1**, 2843 (1994).

[5] A.Y. Aydemir: Phys. Fluids **4**, 3469 (1992).

[6] B.N. Kuvshinov, F. Pegoraro: and T.J. Schep, Phys. Lett. A **191**, 296 (1994).

[7] J. Rem and T.J. Schep: Plasma Phys. and Control. Fusion **40**, 139 (1998).

[8] E. Cafaro, D. Grasso, F. Pegoraro, F. Porcelli, and A. Saluzzi: Phys. Rev. Lett. **80**, 4430 (1998).